Nanophase segregation in binary mixtures of a bent-core and a rodlike liquid-crystal molecule

Chenhui Zhu, Dong Chen, Yongqiang Shen, Christopher D. Jones, Matthew A. Glaser, Joseph E. Maclennan, and Noel A. Clark*

Department of Physics and the Liquid Crystal Materials Research Center, University of Colorado, Boulder, Colorado 80309, USA

(Received 26 October 2009; published 22 January 2010)

We studied mixtures of the achiral bent-core mesogen NOBOW 1,3-phenylene bis[4-(4-9-alkoxyphenyliminonetyl)benzoates] (P-9-O-PIMB) and the small, rodlike liquid crystal 8CB using high-resolution synchrotron x-ray diffraction, freeze fracture transmission electron microscopy, and differential scanning calorimetry. NOBOW and 8CB mix in an isotropic state at high temperatures but phase separate at lower temperatures when NOBOW transforms into the B4 phase and forms chiral helical nanofilaments. In pure NOBOW, the nanofilaments are close packed but at moderate 8CB concentrations, they are separated by nanosized gaps filled by 8CB. At higher concentrations of 8CB, macroscopic phase separation occurs.

DOI: 10.1103/PhysRevE.81.011704 PACS number(s): 61.30.Eb, 64.70.M−

I. INTRODUCTION

Bent-core liquid crystals (LCs) have attracted much attention ever since their recent discovery [1]. Achiral bent-core LC molecules can form polar and chiral phases, in contrast to rodlike molecules, where molecular chirality is necessary to obtain polar ordered and chiral structures. Phases formed out of bent-core molecules have been under intensive investigation, which led to the clear understanding of the B1, B2, and B7 phases [2–4] and very recently the B4 [5] and dark conglomerate phases [6].

Recently, Takanishi *et al.* studied binary mixtures of the achiral bent-core molecule, NOBOW 1,3-phenylene bis[4-(4-8-alkoxyphenyliminonetyl)benzoates] (P-8-O-PIMB) and the well-known rodlike mesogen 5CB [7], in an effort to obtain deeper understanding of the B4 phase. Interestingly, they observed a unique texture below 33 °C, the *I-N* transition temperature of pure 5CB, which they attributed to a new unknown phase, the Bx "phase." Takekoshi *et al.* carried out heat-capacity measurements on the same mixtures and found a c_p anomaly around 33 °C, which they attributed to a transition between two single phases [8]. They proposed that the Bx-B4 transition can be viewed as the *I-N* transition of 5CB molecules in the mixtures which are embedded in a framework of the B4 structure of NOBOW molecules. A more recent work on NOBOW-5CB mixtures showed that the circular dichroism (CD) signal of the B4 phase is greatly enhanced by the embedded 5CB forming helical superstructure with the same handness as the B4 nanofilaments in the Bx phase [9]. However, the exact structure of this new Bx phase was unclear.

In order to understand the Bx phase, we studied mixtures of NOBOW (P-9-O-PIMB, molecular structure in Fig. 3) and 8CB. 8CB has a nematic (*N*) phase like 5CB but also has a smectic-*A* (Sm*A*) phase. The existence of the Sm*A* phase of 8CB allows us to probe the structure of the mixture using high-resolution synchrotron x-ray diffraction. NOBOW-8CB mixtures exhibit a similar Bx texture similar to that reported by the Tokyo group in their mixtures, confirmed by polarizing optical microscopy. Because NOBOW forms very rigorous nanofilament structures which once formed do not change much [5,6], we were able to obtain information about the Bx phase by probing the structure at lower temperature, which turned out to be a phase coexistence of B4 NOBOW and Sm*A* 8CB. Therefore, the Bx phase is essentially a coexistence of B4 NOBOW and nematic 8CB, with the two components showing either nanoscale or macroscopic phase separation.

II. RESULTS AND DISCUSSION

The phase behavior of the mixtures was proved using differential scanning calorimetry (DSC). Pure NOBOW exhibits the isotropic $(I) \rightarrow 169\ ^\circ\mathrm{C} \rightarrow \mathrm{B2} \rightarrow 142\ ^\circ\mathrm{C} \rightarrow \mathrm{B4}$ phase sequence shown in Fig. 1(g). When 10% 8CB is added to pure NOBOW, the I-B2 transition temperature decreases from 169 °C to 158 °C due to freezing point depression. The B2-B4 transition temperature remains at 142 °C because NOBOW and the isotropic 8CB are phase separated [Figs. 1(f) and 1(g)]. When 30% or more 8CB is added, the B2 phase disappears and a direct I-B4 phase transition is observed, as in the studies of Takanishi *et al.* using 5CB [7]. The I-B4 transition temperature decreases monotonically as the 8CB concentration increases due to freezing point depression [Figs. 1(c)–1(e)]. Pure 8CB exhibits the $I \rightarrow 40.3\ ^\circ\mathrm{C} \rightarrow N \rightarrow 33\ ^\circ\mathrm{C} \rightarrow \mathrm{Sm}A$ phase sequence shown in Fig. 1(a). As the 8CB concentration decreases, the *I-N* transition temperature increases and the *N*-Sm*A* transition temperature decreases, slightly broadening the nematic 8CB region [Figs. 2(a)–2(d)]. In addition, the *I-N* peak becomes more rounded and less distinct. Earlier studies of LC in confined geometries, such as 8CB in porous aerogels, showed that the heat-capacity anomaly across the *I-N* transition is suppressed, rounded, and broadened due to the confinement [10]. The observed lowering of the *I-N* transition temperature in such systems was explained by introducing surface disordering effects. On the other hand, some surfaces enhance the ordering, shifting the *I-N* transition to higher temperatures [11]. Since the nematic phase is broadened in the mixtures, the presence of B4 NOBOW must be promoting, rather than hindering, the nematic ordering.

*noel.clark@colorado.edu

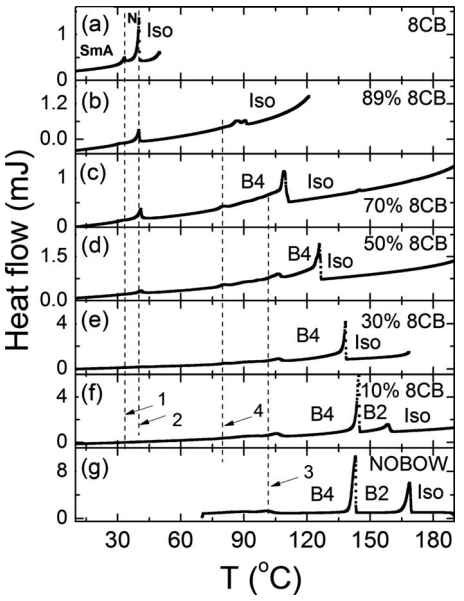

FIG. 1. DSC scans of NOBOW-8CB mixtures (c=10%, 30%, 50%, 70%, and 89%), pure 8CB, and pure NOBOW obtained on cooling. Dashed lines 1, 2, and 3 mark the pure 8CB Sm*A*-N transition, the pure 8CB *I-N* transition, and the pure NOBOW B4 glass transition, respectively. Dashed line 4 marks the prealignment of 8CB into the nematic phase [12]. As the 8CB concentration increases, the transition temperature of the I-B2 transition and the I-B4 transition decreases due to freezing point depression. The nematic range is observed to broaden slightly as the NOBOW concentration increases (see Fig. 2 for an enlarged view).

DSC also shows a small peak at 80 °C for c=30%, 50%, 75%, and 89% (Fig. 1) that is not present in pure bulk NOBOW. Freeze fracture transmission electron microscope (FFTEM) and nuclear magnetic-resonance (NMR) data suggest that 8CB becomes partially aligned by B4 nanofilaments

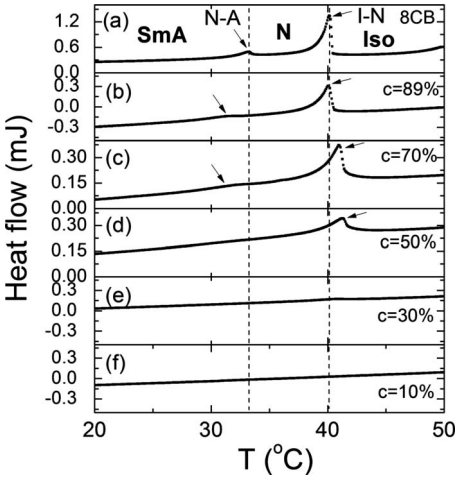

FIG. 2. DSC results of NOBOW-8CB mixtures near room temperature. Dashed lines mark the pure 8CB *N*-Sm*A* and the pure 8CB *I-N* transitions, respectively. The transitions in the mixtures are marked with arrows. As the 8CB concentration decreases, the *I-N* transition temperature increases while the *N*-Sm*A* transition temperature decreases, slightly broadening the 8CB nematic range.

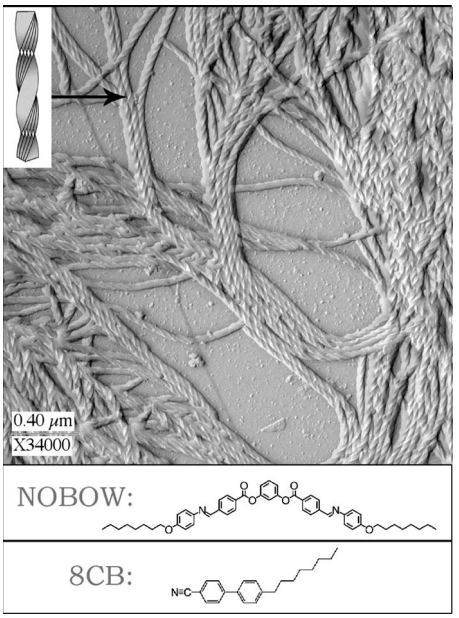

FIG. 3. FFTEM image of the c=75% NOBOW-8CB mixture in the Bx phase. B4 NOBOW forms chiral helical nanofilaments (inset), which develop into an inhomogeneous porous network structure. The sample was first kept in the Bx phase before rapid quenching in liquid propane.

and at this temperature, a surface-induced *I-N* transition occurs [12].

Under the polarized light microscope, the Bx texture appears near the *I-N* transition of 8CB. Similar behavior was also observed in NOBOW-5CB [8] and in NOBOW-$\bar{8}$S5 mixtures [13]. The appearance of the Bx texture must therefore be directly related to the *I-N* transition of the calamitic mesogen.

A FFTEM image of the c=75% mixture in the Bx phase shows that B4 NOBOW forms nanofilaments (36 nm in diameter), some of which form bundles (Fig. 3). The size of nanofilaments does not depend much on c. Apparent voids between the B4 nanofilaments suggest that the structure is porous and inhomogeneous.

High-resolution synchrotron x-ray studies [14] show one x-ray peak at high temperatures and two coexisting x-ray peaks at lower temperatures (below about 33 °C) for c =50%, 70%, and 89% [Fig. 4(b)]. The peak positions are very close to the bulk Sm*A* 8CB peak (q=0.2 Å^{-1}) and the bulk B4 NOBOW peak (q=0.13 Å^{-1}), respectively, strong evidence for the phase coexistence of B4 NOBOW and Sm*A* 8CB. It is also observed that the I-B4 transition temperature decreases as c increases [Fig. 4(b)], in agreement with the DSC results. Since the nematic 8CB phase does not have a layered structure, high-resolution synchrotron x rays are not particularly useful for probing the phase coexistence of B4 NOBOW and nematic 8CB. However, given the rigidity of B4 nanofilaments, we assume the porous network structure of B4 will not change much once it is formed, in particular no difference is expected on cooling 8CB from the isotropic to the Sm*A* phase.

Analysis of the x-ray peaks in the low-temperature region shows that the variation in q (i.e., the layer spacing) of both

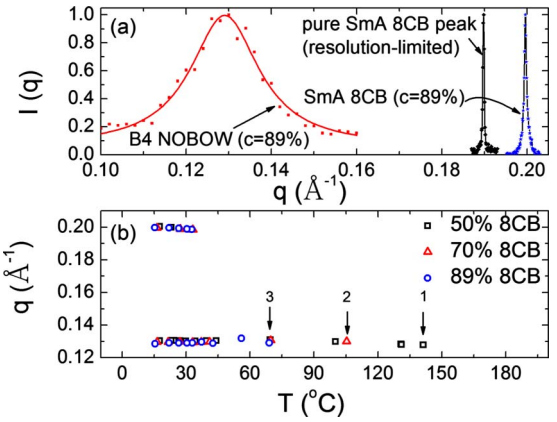

FIG. 4. (Color online) X-ray scattering results for NOBOW-8CB mixtures. (a) The Bx phase in a $c=89\%$ mixture at 25 °C shows the wide B4 NOBOW peak (in red) and the sharp, nanoconfined Sm*A* 8CB peak (in blue). The resolution-limited Sm*A* peak of pure bulk 8CB (in black), sharper than the nanoconfined Sm*A* 8CB peak, is also shown for comparison. Its peak position is shifted leftwards by 0.01 Å^{-1} to help the eye. (b) Layer peak position vs temperature at $c=50\%$, 70%, and 89%. The peak observed near $q=0.13$ Å^{-1} at high temperatures comes from B4 NOBOW. Two peaks are observed near $q=0.2$ Å^{-1} and $q=0.13$ Å^{-1} at lower temperatures, suggesting the phase coexistence of B4 NOBOW and Sm*A* 8CB. As c increases, $T_{\text{I-B4}}$ (arrows 1, 2, and 3 indicate the I-B4 transition for $c=50\%$, 70%, and 89%, respectively) decreases due to freezing point depression.

Sm*A* 8CB and B4 NOBOW with the temperature and concentration is very small, the deviation from the layer spacing of pure bulk 8CB and pure bulk NOBOW being less than 1% in both cases, which practically rules out the possibility of any kind of novel structures, such as those in studies by Pratibha *et al.* [15,16] and by Huang *et al.* [17], for NOBOW-8CB mixtures (Fig. 5). Interestingly, the full width at half maximum (FWHM) of the B4 peak increases while the FWHM of the Sm*A* 8CB peak decreases as the 8CB

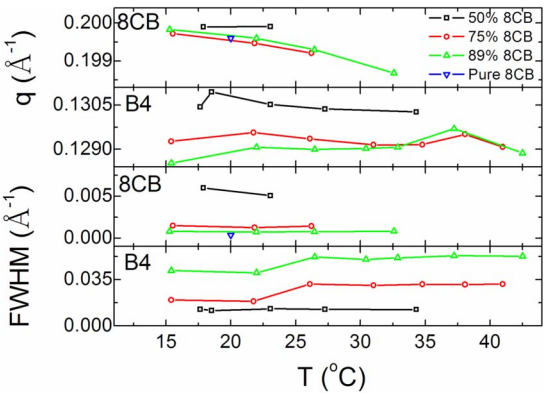

FIG. 5. (Color online) Scattering wave vector q and FWHM of smectic layering peaks vs temperature for different 8CB concentration in NOBOW-8CB mixtures. The q's are essentially no different from those seen in pure bulk Sm*A* 8CB and pure bulk B4 NOBOW, respectively. However, as c increases, the FWHM of the Sm*A* 8CB peak decreases and the FWHM of the B4 NOBOW peak increases, exhibiting a similarity to LC in confined geometries.

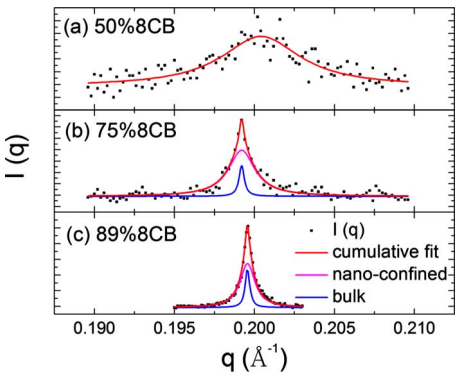

FIG. 6. (Color online) Sm*A* 8CB peak for (a) $c=50\%$, (b) 75%, and (c) 89%. The raw data were fit with two subpeaks: (1) the blue curve corresponding to the bulk 8CB and (2) the magenta curve corresponding to the nanoconfined 8CB. For $c=50\%$, it was impossible to include in any component of the bulk 8CB in the fit. As c increases, the bulk 8CB signal grows, as evidenced by the area under the blue curve.

concentration increases, suggesting a change in the smectic correlation length, $\xi=2/\text{FWHM}$, of both B4 NOBOW and Sm*A* 8CB. For example, ξ_{SmA} increases from 20 nm when $c=50\%$ to 100 nm when $c=89\%$.

The systematic changes in the FWHM of the x-ray peaks and in the DSC transition peak profiles show some similarities to the changes observed in LC in confined geometries, such as 8CB in silica aerogel [18–20]. Silica aerogels are highly porous solids (tens of nanometers pore chord) formed by aggregation and dehydration of suspensions of nm-dimension silica particles. The pores form a continuously connected volume that can be filled with 8CB. It is observed that when the gel density becomes higher, the pore size becomes smaller and the smectic correlation length of the confined 8CB becomes shorter. In addition, due to the existence of cracks (imperfections >1 μm) in the silica aerogel structure, some 8CB is also present in bulk form. The nanoconfined 8CB and bulk 8CB contributions are identified by fitting the overall smectic peak with two subpeaks, one corresponding to each form of 8CB. During fitting, the FWHM of one subpeak is fixed to be the same as that of the pure bulk Sm*A* 8CB peak. The FWHM of the other subpeak is allowed to vary and is typically found to be much wider, corresponding to the shorter correlation length of the nanoconfined Sm*A* 8CB. The general similarities prompted us to perform a similar analysis of our x-ray data.

The Sm*A* 8CB x-ray peak for $c=89\%$, 75%, and 50% was first fit with a single Lorentzian peak to find the peak position, q_0. It was then fit with two subpeaks, centered around q_0, fixing the FWHM of one subpeak to be 0.0004 Å^{-1}, the same as that of pure bulk Sm*A* 8CB. The result is shown in Fig. 6. The magenta curve corresponds to the nanoconfined Sm*A* 8CB and the blue curve corresponds to the bulk Sm*A* 8CB. The areas under each curve are proportional to the volume of each kind of 8CB, with $c=c_{\text{nano8CB}}+c_{\text{bulk8CB}}$. The bulk 8CB component was found to be negligible for $c=50\%$, increasing to about 22% for $c=89\%$ [Fig. 7(b)]. The exact values depend on heating history, for example, the cooling rate, due to the fact that the B4 network formation is a nonequilibrium process.

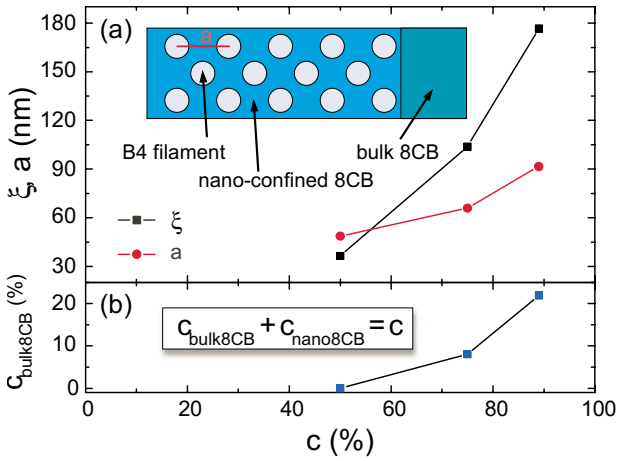

FIG. 7. (Color online) (a) Smectic correlation length ξ of the nanoconfined Sm*A* 8CB and the 2D triangular lattice parameter a of model B4 nanofilament array vs 8CB concentration. Inset schematically shows our model in which 8CB exists in both bulk form and nanoconfined form with NOBOW. The 2D triangular lattice parameter increases as the 8CB concentration increases due to the dilution of B4 nanofilaments by the addition of 8CB. The correlation length of the nanoconfined Sm*A* 8CB increases as the 8CB concentration increases because the space among B4 nanofilaments increases. (b) Bulk form 8CB percentage vs 8CB concentration. At low 8CB concentration, there is no macroscopic phase separation. At $c>50\%$, macroscopic phase separation occurs and the bulk form 8CB component increases as c increases, reaching 22% at $c=89\%$.

We may imagine B4 nanofilaments arranged on a two-dimensional (2D) triangular lattice (with the filaments perpendicular to the lattice plane) and nanoconfined 8CB filling the intervening space [Fig. 7(a)]. The fraction of NOBOW in the mixture is $1-c$, while the fraction of NOBOW in the unit cell is $(1-c)/(1-c_{\text{bulk8CB}})$. The lattice parameter may be determined by computing the fraction of B4 material in the unit cell

$$\frac{\pi r^2}{\frac{\sqrt{3}}{2}a^2} = \frac{1-c}{1-c_{\text{bulk8CB}}},$$

where the radius of B4 nanofilaments, r, is found from FFTEM to be around 18 nm. The relationship of the 2D triangular lattice parameter vs. 8CB concentration and the correlation length of nanoconfined Sm*A* 8CB vs. 8CB concentration are shown in Fig. 7(a). These quantities have roughly the same magnitude and show the same trend with increasing 8CB concentration, verifying our phase-separation model for the NOBOW-8CB mixtures.

III. CONCLUSION

We have carried out high-resolution synchrotron x-ray diffraction, DSC, and FFTEM of binary mixtures of NOBOW-8CB. The Bx phase previously reported in NOBOW-5CB mixtures is proposed to be a nanostructure analogous to the nanophase segregation of B4 NOBOW nanofilaments and nematic 8CB observed in our mixtures. B4 nanofilaments 36 nm in diameter form a porous structure tens of nm in scale which 8CB infiltrates. The nematic 8CB embedded in the porous structure of B4 nanofilaments exhibits the observed Bx texture.

ACKNOWLEDGMENTS

This work was supported by NSF MRSEC Grant No. DMR-0820579. The authors are grateful to D. M. Walba and E. Korblova for materials and H. Takezoe for valuable discussions.

[1] T. Niori, T. Sekine, J. Watanabe, T. Furukawa, and H. Takezoe, J. Mater. Chem. **6**, 1231 (1996).
[2] R. A. Reddy and C. Tschierske, J. Mater. Chem. **16**, 907 (2006).
[3] H. Takezoe and Y. Takanishi, Jpn. J. Appl. Phys. **45**, 597 (2006).
[4] L. E. Hough, C. Zhu, M. Nakata, N. Chattham, G. Dantlgraber, C. Tschierske, and N. A. Clark, Phys. Rev. Lett. **98**, 037802 (2007).
[5] L. E. Hough, H. T. Jung, D. Krüerke, M. S. Heberling, M. Nakata, C. D. Jones, D. Chen, D. R. Link, J. Zasadzinski, G. Heppke, J. Rabe, W. Stocker, E. Körblova, D. M. Walba, M. A. Glaser, and N. A. Clark, Science **325**, 456 (2009).
[6] L. E. Hough, M. Spannuth, M. Nakata, D. A. Coleman, C. D. Jones, G. Dantlgraber, C. Tschierske, J. Watanabe, E. Korblova, D. M. Walba, J. E. Maclennan, M. A. Glaser, and N. A. Clark, Science **325**, 452 (2009).
[7] Y. Takanishi, G. J. Shin, J. C. Jung, S.-W. Choi, K. Ishiwawa, J. Watanabe, H. Takezoe, and P. Toledano, J. Mater. Chem. **15**, 4020 (2005).
[8] K. Takekoshi, K. Ema, H. Yao, Y. Takanishi, J. Watanabe, and H. Takezoe, Phys. Rev. Lett. **97**, 197801 (2006).
[9] T. Otani, F. Araoka, K. Ishikawa, and H. Takezoe, J. Am. Chem. Soc. **131**, 12368 (2009).
[10] L. Wu, B. Zhou, C. W. Garland, T. Bellini, and D. W. Schaefer, Phys. Rev. E **51**, 2157 (1995).
[11] P. Sheng, Phys. Rev. Lett. **37**, 1059 (1976).
[12] D. Chen, C. Zhu, R. Shoemaker, E. Korblova, D. M. Walba, M. A. Glaser, J. E. Maclennan, and N. A. Clark (unpublished).
[13] C. Zhu, Y. Shen, and N. Clark (unpublished).
[14] High-resolution x-ray experiments were done at the beam line X10A at the National Synchrotron Light Source at Brookhaven. The instrument resolution in reciprocal space is ~ 0.0004 Å^{-1}.
[15] R. Pratibha, N. V. Madhusudana, and B. K. Sadashiva, Science **288**, 2184 (2000).
[16] R. Pratibha, N. V. Madhusudana, and B. K. Sadashiva, Phys. Rev. E **71**, 011701 (2005).
[17] M. Y. M. Huang, A. M. Pedreira, O. G. Martins, A. M. Figueiredo Neto, and A. Jákli, Phys. Rev. E **66**, 031708

(2002).

[18] N. A. Clark, T. Bellini, R. M. Malzbender, B. N. Thomas, A. G. Rappaport, C. D. Muzny, D. W. Schaefer, and L. Hrubesh, Phys. Rev. Lett. **71**, 3505 (1993).

[19] T. Bellini, A. G. Rappaport, N. A. Clark, and B. N. Thomas, Phys. Rev. Lett. **77**, 2507 (1996).

[20] T. Bellini, L. Radzihovsky, J. Toner, and N. A. Clark, Science **294**, 1074 (2001).